Research Journal of Applied Sciences, Engineering and Technology 7(24): 5288-5292, 2014
DOI:10.19026/rjaset.7.927
ISSN: 2040-7459; e-ISSN: 2040-7467

Submitted: March 13, 2014 Accepted: April 11, 2014 Published: June 25, 2014

Research Article

New Approach to Determine Vertical Parallel Junction Silicon Solar Cell Parameters

[1]M. Sané, [2]B. Zouma and [1]F.I. Barro
[1]Department of Physics, Semiconductors and Solar Energy Laboratory, Faculty of Science and Technique, Cheikh Anta Diop University, Dakar, Senegal
[2]Department of Physics, Thermal and Renewable Energies Laboratory, Training and Research Unit in Pure and Applied Sciences, University of Ouagadougou, Burkina Faso

Abstract: The aim of this work is to study the electrical behavior of a vertical parallel junction silicon solar cell by mean of impedance spectroscopy. By solving diffusion-recombination equation, the excess minority carrier density expression was established and the photocurrent and the photo voltage were deduced. We plotted Nyquist diagram of the solar cell impedance and gave corresponding electrical circuits. We then introduced impedance spectroscopy method to access for the first time to some electrical parameters of a vertical junction solar cell (series resistance, parallel resistance, capacitance and inductance).

Keywords: Electrical parameters, spectroscopy, vertical junction

INTRODUCTION

The increasing demand for clean energy and the largely untapped potential of the sun as an energy source is making solar energy conversion technology increasingly important. As a result, the demand for solar cells, which convert sunlight directly into electricity, is growing. Solar or Photovoltaic (PV) cells are made up of semiconductor materials that absorb photons from sunlight and then release electrons, causing an electric current to flow when the cell is connected to a load (charge). A variety of measurements are used to characterize a solar cell's performance (Green, 2008; Dieng *et al*., 2011; Kumar *et al*., 2001). In this study, we will lay stress on the impedance spectroscopy (Scofield, 1995; Chenvidhya *et al*., 2005) as a tool for vertical junction electrical characterization; to the best of our knowledge, this is the first time impedance spectroscopy is applied to a vertical junction solar cell. Based on the continuity equation, the excess minority carrier density is derived; from that excess minority carrier density, both photocurrent density and photovoltage are calculated. The vertical junction solar cell impedance is then deduced. By help of Nyquist diagram, electrical circuits of the vertical junction are proposed and from impedance spectroscopy theory, series resistance, parallel resistance, capacitance and inductance are extracted.

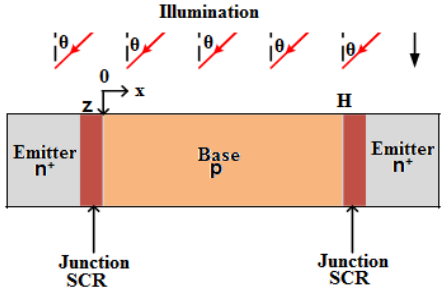

Fig. 1: Vertical junction unit cell

METHODOLOGY

Theoretical development: This study is based on the vertical junction silicon solar cell presented in Fig. 1 with the following assumptions:

- The space charge region and the emitter thicknesses are very small compared to that of the base; their contributions are then neglected so that only the contribution of the base is taken into account (Sissoko *et al*., 1998).
- The emitter and the base regions are quasi-neutrals (Mathieu and Fanet, 2009); there is no internal electric field without the space charge region.
- The electrical and optical properties are identical at any point in the base; this enables us to use the Cartesian coordinates. We also took into account the reflection on the silicon material.

Corresponding Author: F.I. Barro, Department of Physics, Semiconductors and Solar Energy Laboratory, Faculty of Science and Technique, Cheikh Anta Diop University, Dakar, Senegal

- The temperature effect on the performance of the photovoltaic cell is not taken into account.
- The excitation is done with a monochromatic frequency modulated light. The incident photons flux ϕ (λ) is taken for AM 1.5 solar spectrum (Green, 2008). This case is characteristic of the whole terrestrial applications independently of the processing site.

Excess minority carrier density: Taking into account generation, recombination and diffusion phenomena in the base, the equation governing the variation of the minority carriers density δ (x, y, z, t) under frequency modulation (Dieng *et al*., 2011) is:

$$D(\omega)\cdot\frac{\partial^2\delta(x,\theta,t)}{\partial x^2}-\frac{\delta(x,\theta,t)}{\tau}= -G(z,\theta,t)+\frac{\partial\delta(x,\theta,t)}{\partial t} \quad (1)$$

D (ω) and τ are, respectively the excess minority carrier diffusion coefficient and lifetime.

The excess minority carrier density can be written as:

$$\delta(x,t)=\delta(x)\exp(-j\omega t) \quad (2)$$

The excess minority carrier generation rate is given by Dieng *et al*. (2011):

$$G(z,\theta,\lambda,t)=g(z,\theta,\lambda)\exp(-j\omega t) \quad (3)$$

were,

$$g(z,\theta,\lambda)=\alpha(\lambda)(1-R(\lambda))\cdot\phi(\lambda)\cdot \exp(-\alpha(\lambda)\cdot z)\cdot\cos(\theta) \quad (4)$$

x = The base depth along x axis
ω = The angular frequency
θ = The incidence angle
z = The base depth according to the vertical axis
λ = The illumination wavelength

If we replace Eq. (2) into (1), the temporal part is eliminated and we obtain:

$$\frac{\partial^2\delta(x)}{\partial x^2}-\frac{\delta(x,\theta,t)}{L(\omega)^2}=-\frac{g(z,\theta)}{D(\omega)} \quad (5)$$

The solution of this equation is in the form:

$$\delta(x,\omega,\theta,z,Sf,\lambda)=A\cosh\left(\frac{x}{L(\omega)}\right)+B\sinh\left(\frac{x}{L(\omega)}\right) +\frac{L(\omega)^2}{D(\omega)}\cdot\alpha(\lambda)(1-R(\lambda))\cdot\phi(\lambda)\cdot \exp(\alpha(\lambda)\cdot z)\cdot\cos(\theta) \quad (6)$$

Coefficients A and B is determined through the following boundary conditions (Dieng *et al*., 2011):

- At the junction (x = 0):

$$D(\omega)\cdot\left.\frac{\partial\delta(x,\omega,\theta)}{\partial x}\right|_{x=0}=Sf\cdot\delta(x,\omega,\theta)\Big|_{x=0} \quad (7)$$

  Sf is related to the carrier flow through the junction (Diallo *et al*., 2008).
- At the middle of the base (x = H/2):

$$D(\omega)\cdot\left.\frac{\partial\delta(x,\omega,\theta)}{\partial x}\right|_{x=\frac{H}{2}}=0 \quad (8)$$

Photocurrent density: The main contribution to the photocurrent Jph comes from diffusion; Jph can be written in the form:

$$J_{Ph}=2\cdot q\cdot D(\omega)\cdot\left.\frac{\partial\delta(x,\omega,\theta)}{\partial x}\right|_{x=0} \quad (9)$$

q is the elementary charge.

The factor 2 results from the two junctions around the base and the fact that they are connected in a parallel manner.

Photo voltage: According to the Boltzmann's relation, the photo voltage is given by Sze and Ng. Kwok (2007) and Hu (2010):

$$V_{Ph}=V_T\cdot\ln\left[1+\frac{Nb}{n_0^2}\cdot\delta(0)\right] \quad (10)$$

With V_T the thermal voltage, Nb the base doping density and n_0 the intrinsic carrier density.

Impedance: The vertical junction solar cell's impedance may be defined by Kumar *et al*. (2001) and Dieng *et al*. (2011):

$$Z(\omega,\theta,z,Sf,\lambda)=\frac{V_{ph}(\omega,\theta,z,Sf,\lambda)}{J_{ph}(\omega,\theta,z,Sf,\lambda)} \quad (11)$$

The corresponding Nyquist diagram i.e., the representation of imaginary part of the complex function Z (ω, θ, z, Sf, λ) versus its real part (Kumar *et al*., 2001; Chenvidhya *et al*., 2003; Chenvidhya *et al*., 2005):

$$\mathrm{Im}(Z(\omega,\theta,z,Sf,\lambda))=f(\mathrm{Re}(Z(\omega,\theta,z,Sf,\lambda))) \quad (12)$$

RESULTS AND DISCUSSION

We plotted in Fig. 2a and 3a the Nyquist diagram of the vertical junction impedance; the obtained curves

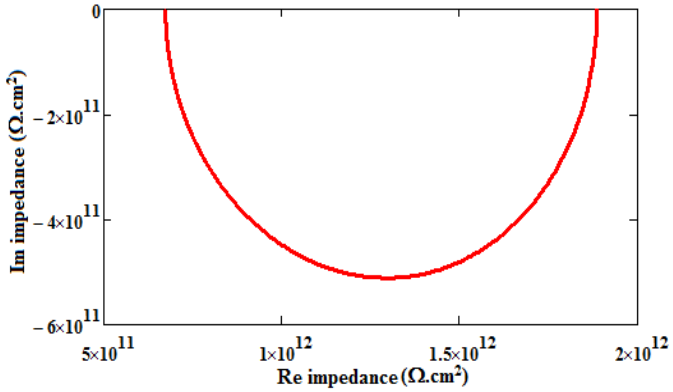

(a)

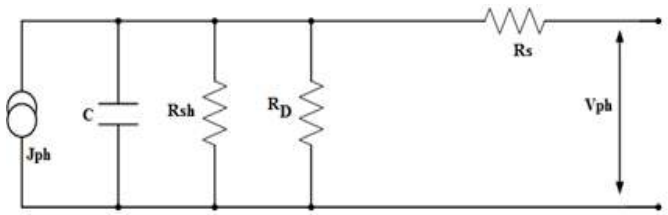

(b)

Fig. 2: (a) Nyquist diagram, (b) electrical circuit of solar cell for capacitive effects
Sf: 3.10^3 cm/sec; H: 0.03 cm; Lo: 0.02 cm; z: 0.0001 cm; Do: 26 cm²/sec; λ: 0.5 µm

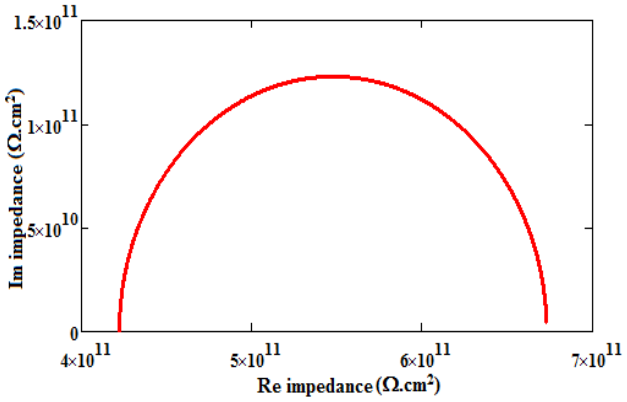

(a)

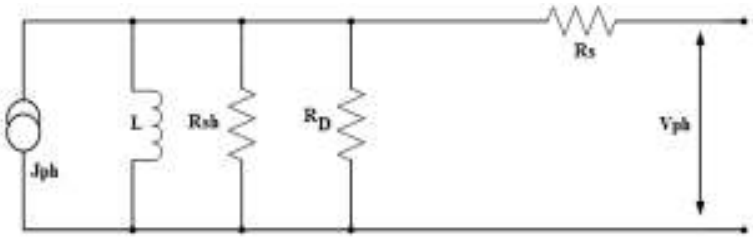

(b)

Fig. 3: (a) Nyquist diagram, (b) electrical circuit of solar cell for inductive effects
Sf: 3.10^3 cm/sec; H: 0.03 cm; Lo: 0.02 cm; z: 0.0001 cm; Do: 26 cm²/sec; λ: 0.5 µm

are semi-circles of two types: positive one and negative one depending on incidence angle value. For the negative one (Fig. 2a) the parallel vertical junction behaves inductively contrary to the curve in Fig. 3a where capacitance phenomenon predominates.

From these two behavior the vertical junction solar cell can be represented by one of the electrical circuit presented on Fig. 2b and 3b:

- C is the total capacitance; $C = C_T + C_D$ where C_D is the diffusion capacitance due to the diffusion of the excess minority carrier density in the base and C_T is the transition capacitance due primarily to the fixed atoms ionized in the space charge region.
- Rsh models leakage currents existing at the edge of the structure, the whole of the defects in the vicinity of the space charge region (dislocation, recombination centers) and in the base.
- R_D is the solar cell dynamic resistance, it indicate the local behavior of the solar cell for a given operating conditions.
- Rs is the series resistance related to material resistivity and metallization grid.
- L is related to the inductive behavior of the cell; it comes from the frequency effects through low resistances particularly the quasi-neutrals regions and metallization.

Both capacitive and inductive effects play very important role in determining solar cell parameters (like under flashed irradiance and transient experiments) and in switching circuits with power inverters.

Impedance spectroscopy technique: If we consider for example the capacitive behavior the cell with the associated electrical circuit of Fig. 2b, the impedance Z is given by Rs in series with Zc parallel to Rp; $Rp = Rsh//R_D$, $Zc = 1/(jc\omega)$. For the circuit of Fig. 3b, the following calculations remain valid if Zc is replaced by $Z_L = jL\omega$.
We then have:

$$Z = R_S + \left(\frac{1}{R_p} + \frac{1}{Z_C}\right)^{-1} \tag{13}$$

If we replace Rp and Zc by their expressions and after some calculations, we obtain:

$$Z = R_S + \frac{R_D \cdot R_{Sh} \cdot (R_D + R_{Sh})}{(R_D + R_{Sh})^2 + (\omega \cdot R_D \cdot R_{Sh} \cdot C)^2} - \frac{j \cdot \omega \cdot (R_D \cdot R_{Sh})^2 \cdot C}{(R_D + R_{Sh})^2 + (\omega \cdot R_D \cdot R_{Sh} \cdot C)^2} \tag{14}$$

Z is a complex number which real part Re (Z) and imaginary part Im (Z) are given by:

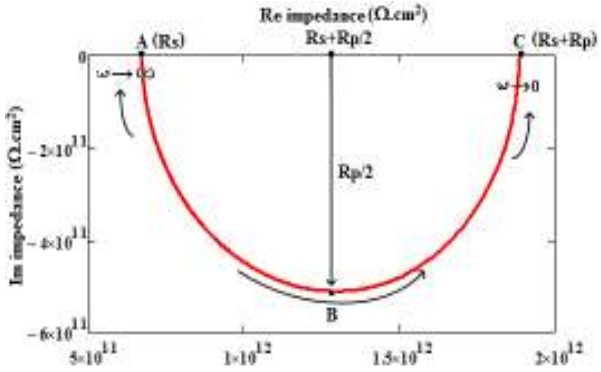

Fig. 4: Nyquist diagram with the particular points
Sf: 3.10^3 cm/sec; H: 0.03 cm; Lo: 0.02 cm; z: 0.0001 cm; Do: 26 cm²/sec; λ: 0.5 μm; θ: 48.2°

$$\mathrm{Re}(Z) = R_S + \frac{R_D \cdot R_{Sh} \cdot (R_D + R_{Sh})}{(R_D + R_{Sh})^2 + (\omega \cdot R_D \cdot R_{Sh} \cdot C)^2} \tag{15}$$

From the equations above, several particular cases can be considered according to the modulation frequency on one hand and to the ratio of R_D and Rsh:

- If $\omega \to 0$, the imaginary part Im (Z) of Z is null and only the real part Re (Z) remains:

  $Re(Z) = Rs + R_D \cdot Rsh / (R_D + Rsh)$

  The impedance is rewritten in the form:

  $Z = Rs + R_D \cdot Rsh / (R_D + Rsh)$

  - If $Rsh >> R_D$ we have $Re(Z) = Rs + R_D$ and the impedance Z is reduced to: $Z = Rs + R_D$
  - If $Rsh << R_D$ then one has $Re(Z) = Rs + Rsh$ and thus $Z = Rs + Rsh$
- If $\omega \to \infty$ the imaginary part Im (Z) of Z is also null and we have: Re (Z) = Rs

The impedance can then is measured in the form: Z = Rs independently of the ratio of Rsh and R_D.

Taking into consideration these calculations, if we return to the Nyquist diagram itself, we can associate some particular points depending on the modulation frequency (Dieng *et al*., 2011) as presented in Fig. 4.

The Nyquist diagram corresponds to a semi-circle of radius Rp/2 and center (Rp/2+Rs, 0). A correspond to low modulation frequency ($\omega \to 0$) and C to higher modulation frequencies ($\omega \to \infty$). That is, some electrical parameters can be determined the mean of the technique described above.

Appling the impedance spectroscopy, we obtain (Table 1).

To determine the associated capacitance, let us consider the following equation obtained thanks to the cut-off frequency:

Table 1: Series and parallel resistances capacitive behavior

Rs ($\Omega.cm^2$)	$6{,}7318.10^{-3}$
Rp ($\Omega.cm^2$)	$1{,}254.10^{3}$

Table 2: Series and parallel resistances inductive behavior

Rs ($\Omega.cm^2$)	$4{,}2225.10^{-3}$
Rp ($\Omega.cm^2$)	$2{,}508.10^{3}$

$$\tau_C = R_p \cdot C = \frac{2\pi}{\omega_C} \tag{16}$$

That leads to C = $5{,}011.10^{-8}$ µF.

In the case of an inductive behavior, we have (Table 2).

The associated inductance is deduced from Eq. (17):

$$\tau_L = R_p \cdot L = \frac{2\pi}{\omega_c} \tag{17}$$

This leads to L = $2{,}505/10^{8}$ µH.

CONCLUSION

Based on an ac-equivalent circuit of a parallel vertical junction solar cell, an expression of the impedance has been established. From Nyquist diagram, we presented two electrical circuits of the solar cell. The impedance spectroscopy technique is then applied to extract for the first time the vertical junction electrical parameters.

REFERENCES

Chenvidhya, D., K. Kirtikara and C. Jivacate, 2003. A new characterization method for solar cell dynamic impedance. Sol. Energ. Mat. Sol. C., 80: 459-464.

Chenvidhya, D., D. Kirtikara and C. Jivacate, 2005. PV module dynamic impedance and its voltage and frequency dependencies. Sol. Energ. Mat. Sol. C., 86(2) pp: 243-251.

Diallo, H.L., A. Wereme, A.S. Maiga and G. Sissoko, 2008. New approach of both junction and back surface recombination velocities in a 3D modelling study of a polycrystalline silicon solar cell. Eur. Phys. J-Appl. Phys., 42: 203-211.

Dieng, A., I. Zerbo, M. Wade, A.S. Maiga and G. Sissoko, 2011. Three-dimensional study of a polycrystalline silicon solar cell: The influence of the applied magnetic field on the electrical parameters. Semicond. Sci. Tech., 26(095023): 9.

Green, M.A., 2008. Self-consistent optical parameters of intrinsic silicon at 300K including temperature coefficients. Sol. Energ. Mat. Sol. C., 92: 1305-1310.

Hu, C.C., 2010. Modern Semiconductor Devices for Integrated Circuits. Pearson/Prentice Hall, New Jersey.

Kumar, R.A., M.S. Suresh and J. Nagaraju, 2001. Measurement of AC parameters of gallium arsenide (GaAs/Ge) solar cell by impedance spectroscopy. IEEE T. Electron. Dev., 48(9): 2177-2179.

Mathieu, H. and H. Fanet, 2009. Physique des Semi-Conducteurs et Des Composants Electroniques. 6th Edn., Dunod, Paris.

Scofield, J.H., 1995. Effects of series resistance and inductance on solar cell admittance measurements. Sol. Energ. Mat. Sol. C., 37(2): 217-233.

Sissoko, G., E. Nanema, A. Correa, M. Adj, A.L. Ndiaye and M.N. Diarra, 1998. Recombination parameters measurement in double sided surface field solar cell. Renew. Energ., 3 : 1856-1859.

Sze, S.M. and K. Ng. Kwok, 2007. Physics of Semiconductors Devices. Wiley, New York.